

Heterogeneities in systems with quenched disorder

Mendeli H Vainstein¹, Daniel A Stariolo^{2,3} and Jeferson J Arenzon^{2,3}

¹ Instituto de Física, UnB, CP 04455, 70919-970 Brasília, DF, Brazil

² Instituto de Física, UFRGS, CP 15051, 91501-970 Porto Alegre RS, Brazil

E-mail: mendeli@iccmp.br, stariolo@if.ufrgs.br and arenzon@if.ufrgs.br

Received 14 April 2003

Published 15 October 2003

Online at stacks.iop.org/JPhysA/36/10907

Abstract

We study the strong role played by structural (quenched) heterogeneities on static and dynamic properties of the frustrated Ising lattice gas in two dimensions, already in the liquid phase. Different from the dynamical heterogeneities observed in other glass models, in this case they may have infinite lifetime and be spatially pinned by the quenched disorder. We consider a measure of local frustration to show how it induces the appearance of spatial heterogeneities and how this reflects in the observed behaviour of equilibrium density distributions and dynamic correlation functions.

PACS numbers: 05.50.+q, 61.43.Fs

1. Introduction

Much of the work in the theory of the glass transition has been concentrated in the precursor phenomena present in the high temperature (or low density) phase on approaching the glass transition. The (equilibrium) dynamics in this region shows two qualitatively different regimes: a short time relaxation associated with the rattling of particles inside cages formed by their neighbours and a long time structural relaxation which, as density increases (or T decreases), takes longer and longer times [1, 2]. In supercooled liquids, the presence of a crossover temperature below which exponentially decaying correlation functions typical of the liquid phase become stretched has been observed [3]. The origin of this stretching of relaxations is associated with the gradual appearance of heterogeneities in the space/time domain. Understanding the emergence of these heterogeneities is at the heart of the nature of the glass transition and has been the source of a lot of theoretical and experimental work [4–6]. Nevertheless, a unifying microscopic theory is still lacking and only a few universal properties related to heterogeneities have been found.

³ Associate researcher of the Abdus Salam International Centre for Theoretical Physics.

In real space, dynamical heterogeneities correspond to particles with different mobilities. In computer simulations of simple glass formers the presence of *fast* and *slow* particles has been observed. The typical time scales of the two types of particles can be identified for example by examining the behaviour of the non-Gaussian parameter associated with the van Hove correlation function [7, 8]. This leads to the identification of a growing time scale which seems to diverge at the mode coupling transition temperature (T_{MCT}). This characteristic time arises naturally when computing a suitable time dependent four point correlation function or *dynamical non-linear susceptibility* [9, 10]. As the temperature approaches T_{MCT} from above, this dynamical response shows a growing peak at a characteristic time t^* and then relaxes at long times to its equilibrium value. This growing characteristic time of the four point functions has been associated with the presence of long lived dynamical heterogeneities (clusters of very slow or immobile particles).

From a landscape point of view, the emergence of stretching seems to be the consequence of the gradual confinement of the system in low (free) energy regions of phase space surrounded by growing barriers as temperature decreases. The confinement is due in part to the dramatic decrease of escape directions in configuration space on approaching the glass transition [11–13]. In simple models of binary mixtures it has been found that stretched relaxations are associated with long lived superstructures or ‘metabasins’ in configuration space [14]. The relaxation from single metabasins shows a stretched behaviour and different metabasins relax with different characteristic times, giving rise to the overall stretching observed for example in the α region of the incoherent scattering function.

At variance with the enormous amount of work on the problem of heterogeneities in glasses, much less is known about them in systems with quenched disorder [15–18]. Different from true glasses, where the inhomogeneities are dynamically created by the self-induced local frustration and persist during a given timescale, the quenched disorder induces structural heterogeneities that may have infinite lifetime. In this sense they can be called *quenched heterogeneities*. Since the inhomogeneities are pinned by the disorder, they may be easier to detect and characterize than in systems with self-induced disorder. Thus, the posed question is to what extent these heterogeneities influence the relaxation properties and how different regions of the sample differ from each other. Moreover, how do they affect the different degrees of freedom present in the system (such as particles and spins)?

To answer these questions, in this work we address the problem of heterogeneities in systems with quenched disorder by focusing the analysis on the behaviour of a two-dimensional version of the frustrated Ising lattice gas (FILG) which has been proposed as a simple lattice glass model [19]. Nevertheless, it is known that the presence of quenched disorder in the definition of the model introduces some features not typical of real glasses. In particular, it acts as a pinning field for heterogeneities, some of which can have infinite lifetime. This is reflected in the behaviour of dynamical correlation functions and in the non-linear susceptibility and compressibility as will be shown below. In this context we will consider a measure of local frustration, and show how it induces the appearance of spatial heterogeneities and how this reflects in the observed behaviour of equilibrium density distributions and dynamic correlation functions. For the sake of comparison with other glassy systems without quenched disorder we also discuss the behaviour of the non-linear susceptibility associated with the spin degrees of freedom and of the non-linear compressibility of the density variables. Finally, an analysis of the universal behaviour in terms of hole variables recently introduced [20, 21] shows that this system seems to be in a different universality class than the previously investigated glass models without disorder.

2. The model

The frustrated Ising lattice gas [19, 22–24] is defined by the Hamiltonian

$$H = -J \sum_{(ij)} (\varepsilon_{ij} \sigma_i \sigma_j - 1) n_i n_j - \mu \sum_i n_i \quad (1)$$

where $J \rightarrow \infty$. At each site of the lattice there are two different dynamical variables: local density (occupation) variables $n_i = 0, 1$ ($i = 1, \dots, N$) and internal degrees of freedom, $\sigma_i = \pm 1$. The usually complex spatial structure of the molecules of glass forming liquids, which can assume several spatial orientations, is in part responsible for the geometric constraints on their mobility. Here we consider the simplest case of two possible orientations, and the steric effects imposed on a particle by its neighbours are felt as restrictions on its orientation due to the quenched variables ε_{ij} connecting nearest neighbour sites. The first term of the Hamiltonian ensures that when J is large, any two neighbouring particles will have their spins satisfying the connection between them. Finally μ represents a chemical potential ruling the system density (at fixed volume).

This model has been studied mainly through simulations [19, 22, 24] in 3d and analytically in mean field [25, 26]. In the low density (high temperature) phase, the system behaviour is liquid like, the dynamics is fast, time-translationally invariant and obeys the fluctuation–dissipation theorem. By increasing the density (or lowering the temperature), the system has a spin glass transition characterized by a divergence of the static nonlinear susceptibility. In terms of density, this transition point is located quite close to the point where the system suffers a dynamical arrest, and where the particles are no longer able to diffuse. After a sub-critical quench, the dynamics is slow and history dependent. Besides this, it presents ageing and violates the fluctuation–dissipation theorem (we refer the interested reader to [24] and references therein).

3. Static properties

Since bonds are created at random (with probability 1/2 of being ± 1), the system is not homogeneous at the lengthscale of the lattice spacing. Each site belongs to several minimal plaquets and there is a probability that all (or neither) of these are frustrated. This would influence the dynamics at a local level since the system is no longer invariant under spatial translations. Thus we may ask which are the consequences of these quenched heterogeneities on the equilibrium properties of the system.

When evaluating the partition function for the $J \rightarrow \infty$ case at finite density, the configurations in which particles close any frustrated loop will have zero probability. The average density will no longer be site independent and the density distribution $P(\rho)$ will be inhomogeneous, i.e. will show spatial fluctuations. Homogeneity will only be recovered when $\rho \rightarrow 0$. For small densities, the distribution will be Gaussian while deviations from Gaussianity should be evident as the density increases. The forbidden configurations introduce spatial inhomogeneities that are long lived as they derive from the quenched *random* underlying connections. In other lattice models, as well as in structural glasses, the disorder is not quenched, which restores translational invariance if the measure time is much larger than the dynamical heterogeneities characteristic time. An example of a system with quenched but not random frustration that does not present these inhomogeneities is the fully frustrated version of the FILG.

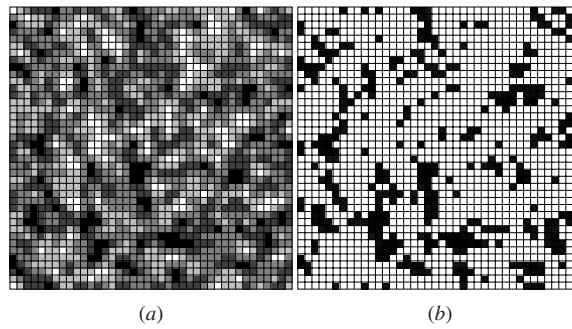


Figure 1. (a) Example of a $\{\gamma_i\}$ configuration. Black sites are those whose four neighbour plaquets are non-frustrated ($\gamma_i = 4$) while white sites have all frustrated ($\gamma_i = -4$). Intermediate values of γ_i are represented by different degrees of grey. (b) Sites whose average density is higher than 0.9 for $\mu = 4$, corresponding to a global $\rho \simeq 0.74$.

To quantify this we use the (local) coarse-grained quantity [15, 17]

$$\gamma_i \equiv \sum_{\mathcal{P}(i)} \prod_{j \in \mathcal{P}(i)} \varepsilon_{ij} \quad (2)$$

where $\mathcal{P}(i)$ are the minimal plaquets containing the site i . That is, for every site, we consider the four minimal plaquets that contain that site (12 in $d = 3$) and we check how many of these plaquets are frustrated, i.e. the product of the connections in the loop is negative. In this nearest neighbour plaquet, approximation sites that are maximally frustrated have all of its four plaquets with negative products and sites with no frustration have all plaquets with positive products. In other words, γ_i may assume values between -4 and 4 . Figure 1(a) shows a configuration with inhomogeneous distribution of local frustration.

We now consider how these structural clumps change the system's behaviour. In figure 1(b) we show, for the same realization of disorder of figure 1(a), only the sites that have an averaged occupation greater than 0.9. In this figure, $\mu = 4$, and the total average density is roughly 0.74, well below 0.9. The presence of preferred positions is a direct consequence of the existence of islands of low frustration, as can be seen by comparing figures 1(a) and (b). As the chemical potential increases, the number of these sites also increases, as expected. These heterogeneities make the system not translationally invariant even in the low density liquid phase. This can be made clear by measuring the distribution $P(\rho_i)$ of local averaged densities $\rho_i = \langle n_i \rangle$ as shown in figure 2. In homogeneous systems all sites have the same average density and the distribution, for a finite number of measurements, is a Gaussian centred in this value. Examples might be a non-disordered version of the model considered here (with fully frustrated connections) or models for structural glasses without quenched variables. In the last case, the annealed character of the frustration allows the homogeneity to be recovered again. The broadness of the curves does not seem related either to finite average times or to finite lattice sizes, but rather to the fact that, when not limited to the nearest neighbour plaquet approximation, there are several values that the local frustration may assume generating in this way the broad distributions seen in the above figures.

To make clear the origin of this broad distribution, we considered the density distribution $P(\rho_i, \gamma_i)$ separately for each value of the local frustration γ_i , which has a well-defined density around which its particular distribution is centred. The result is seen in figure 3. Moreover, the separation between these curves increases as the density increases and the deviation from

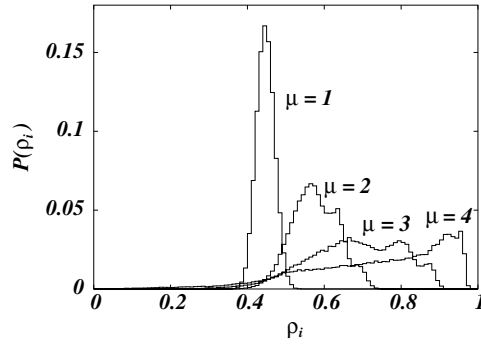


Figure 2. Distribution of local densities for several values of μ and $L = 20$ in 2d. Notice the multi-peak structure that becomes more apparent as μ increases.

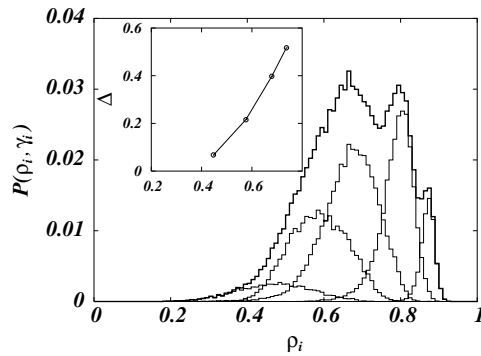


Figure 3. Distribution of local densities for $\mu = 3$ and $L = 20$ in 2d. The bold curve is the sum of several others, $P(\rho_i)$. From left to right, we have 4, 3, \dots , 0 locally frustrated loops. The distribution has an internal structure. Inset: The distance Δ between the average densities for extreme values of γ , $P(\rho_i, 4)$ and $P(\rho_i, -4)$.

Gaussianity becomes apparent. We may define Δ as the difference between the average densities of the peaks associated with the lowest and highest values of γ , $\Delta \equiv \langle \rho_i \rangle_4 - \langle \rho_i \rangle_{-4}$ where the averages $\langle \dots \rangle_{\gamma_i}$ are over $P(\rho_i, \gamma_i)$. When there is no difference, $\Delta = 0$, the particles do not feel the underlying landscape and all sites have the same average equilibrium density. In this model this happens for very low densities. As the density increases, the dynamics becomes landscape influenced and $P(\rho_i)$ has a more complex structure, no longer being a simple Gaussian. This is exemplified in figure 3 for $\mu = 3$. One can also note that the distributions are asymmetric around $\gamma_i = 0$: for example, in the case of $P(\rho_i, -2)$ and $P(\rho_i, 2)$ the former is broader and shorter while the latter is higher and more concentrated. A possible explanation is that sites with negative values of γ_i are more influenced by higher order plaquets than sites with positive γ_i , thus having a broader distribution.

In $d = 3$ the overall picture is similar to that of $d = 2$. Nevertheless, some differences are evident when comparing figures 2 and 4 and one may wonder if the minimum plaquet approximation used in the definition of the local frustration parameter works in $d = 3$ as it does in $d = 2$. Still within the same approximation, the distribution of local densities for different local frustrations presents also different peaks (not shown), a manifestation of the lack of translational invariance also in $d = 3$.

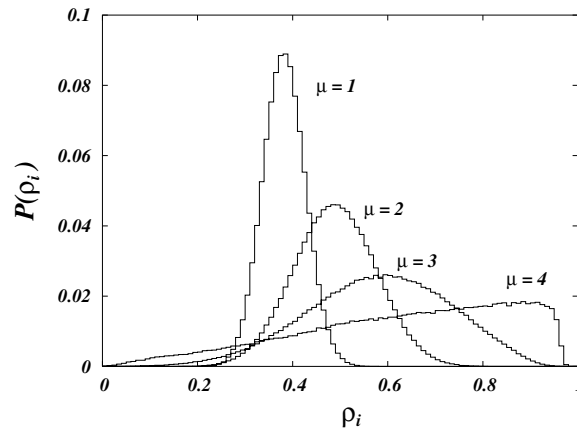


Figure 4. Distribution of local densities for several values of μ and $L = 10$ in 3d. Different from the 2d case, the curves do not seem to present internal structure.

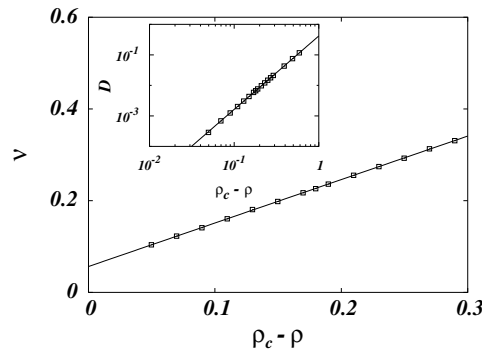


Figure 5. The fraction of holes ν as a function of $\rho - \rho_c$ for $L = 50$. Note that ν does not vanish at $\rho_c \simeq 0.79$. The behaviour near ρ_c is linear with the density. Inset: diffusion coefficient as a function of $\rho_c - \rho$. The diffusivity goes to zero as $(\rho_c - \rho)^\phi$ with $\phi \simeq 2.4$.

Recently, a description of the jamming transition has been introduced that unveiled some universal mechanism leading to the dynamical arrest that happens at ρ_c . The notion of hole is introduced: empty sites that have at least one neighbour particle able, due to the energetic or to the kinetic constraints, to jump to the initial empty site. We measure, for several *fixed* densities⁴ the density of holes, ν . It has been conjectured, and supported by numerical simulations on some lattice models [20, 21], that the diffusivity depends on ν as $D \sim (\nu - \nu_0)^2$ where ν_0 is a possible residual density of holes at ρ_c (rattlers) that do not contribute to the diffusion. We show our results for the FILG in $d = 2$ in figure 5. We obtain $D \sim (\nu - 0.056)^{2.4}$. The Kob–Andersen is another example of model where $\nu_0 \neq 0$. Some things are remarkable: first, we note that the FILG belongs to a different universality class. Second, the value of ν at ρ_c is much larger than in other models. Note also that the behaviour of ν near ρ_c is linear. The fact that the FILG does not belong to the same universality class of several other models is very interesting and the reason may be related to the inhomogeneity of the underlying connections structure. Indeed, we measure the density of holes accordingly

⁴ In this case, when diffusing, the particle carries its spin.

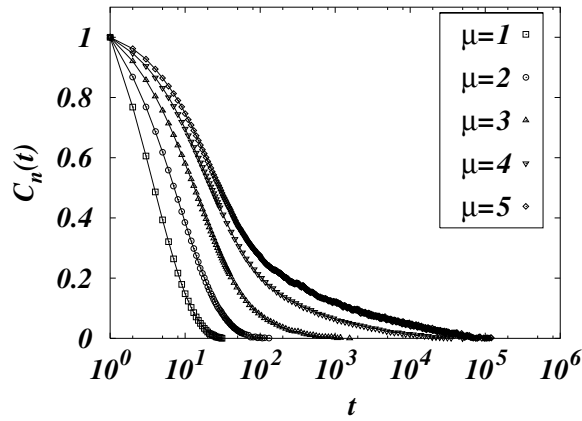


Figure 6. Equilibrium particle correlations $C_n(t)$ for several values of μ for a dynamics with spin flip, particle creation–destruction and diffusion.

to the γ_i of the hole site. For small values of ρ there is no difference between these values and all curves collapse. The fact that for higher densities these curves fall apart is an indication that the holes also have preferred sites and tend to form small clusters. Thus, near ρ_c , the mechanism leading to diffusion is no longer the pairwise collisions between holes but a more complicated process involving these small clusters, which may lead to a failure of the ν -square law⁵. Further work along this line has to be done in order to clarify this issue.

4. Dynamical properties

In [23] the non-equilibrium behaviour of the model was shown to present interesting ageing properties similar to those observed in glass forming systems. Here we address equilibrium density correlations instead and the role of heterogeneities in the low density phase. The density autocorrelations are defined by

$$c_n(t) = \frac{1}{N} \sum_i [\langle n_i(t)n_i(0) \rangle - \langle n_i(0) \rangle^2] \quad (3)$$

and $C_n(t) \equiv c_n(t)/c_n(0)$, where the averages are both over samples and initial states. The densities are also averaged over the thermal history in each sample. Note that only in the case where the system is homogeneous, that is, the average quantities are invariant under spatial translations, we can substitute the last term in the numerator by ρ^2 , otherwise $\sum_i \langle n_i \rangle^2 \neq \langle \sum_i n_i \rangle^2$. In the region of densities considered here, these correlations do not present the usual two step dynamics observed in other models as can be seen in figure 6. Nevertheless, two regimes can be clearly observed and all the curves can be fitted by stretched exponentials (not shown) in the first regime. The second regime at longer times observed for the largest densities can also be fitted by stretched exponentials with other parameters and probably will tend to develop a plateau at higher densities.

⁵ Deviations from this law were also observed in the KA model in the density regime near the dynamical arrest (M Sellitto, private communication).

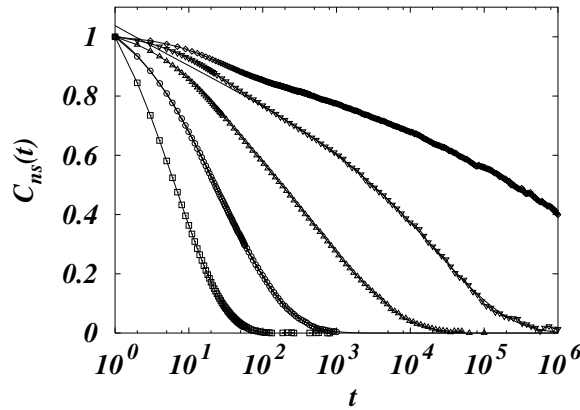


Figure 7. Equilibrium diluted spin correlations $C_{ns}(t)$ for several values of μ for a dynamics with spin flip, particle creation–destruction and diffusion. The symbols are the same as in figure 6.

For the same values of the chemical potential or mean density shown in figure 6, the diluted spin correlations show a different behaviour. The correlations between spins on occupied sites are defined as

$$C_{ns}(t) = \frac{1}{N} \sum_i \langle n_i(t) S_i(t) n_i(0) S_i(0) \rangle. \quad (4)$$

The results for several values of μ are shown in figure 7 together with the best fits to stretched exponential decays for the long time regime. Interestingly, the correlations C_n and C_{ns} decay with very different timescales: density correlations decay much faster than the diluted spin correlations. This can be understood as follows. Particles can be created/destroyed and diffused through the lattice, forming clusters of neighbouring particles. Once they belong to the same cluster, the nature of the interaction enforces them to have spins satisfying all the bonds in the cluster, otherwise they should move apart. Thus, when a site contributes for the correlation at different times, the contribution will be positive, unless there is enough time for the whole cluster to flip all its spins. Moreover, the percolation transition is just below $\mu = 3$ and the considered clusters are large, making the decorrelation time quite large. The diluted spin correlations start to develop an incipient plateau as the value of the chemical potential increases. We expect that by further increasing the value of μ , this plateau will be more noticeable and the characteristic decay time will tend to diverge at the dynamical transition. In figure 8 we show an Arrhenius plot of the relaxation times showing that they tend to diverge for $\mu \rightarrow \infty$. This is different from the behaviour observed in the three-dimensional model [27], which shows a power law divergence at a finite value of μ . Thus, while the three-dimensional model presents a spin glass transition at a finite chemical potential, the two-dimensional model only has a transition at $\mu \rightarrow \infty$.

Both correlations can also be measured only for sites presenting a given value of the frustration parameter γ_i . The curves for the five possible values (in $d = 2$) are shown in figures 9 and 10 for $\mu = 3$. Fits to stretched exponential decay are also shown for the diluted spin correlations. They are normalized to unity but, recalling figure 3, the number of sites contributing to each one of the curves is different. The behaviour for $C_n(t)$ is very different and almost all curves give the same correlation, only sites with $\gamma_i = 4$ differ slightly from the others (and their contribution to the overall curve is small). On the other hand, for $C_{ns}(t)$ the curves are strongly resolved and we note that the dynamics is faster in those sites in highly

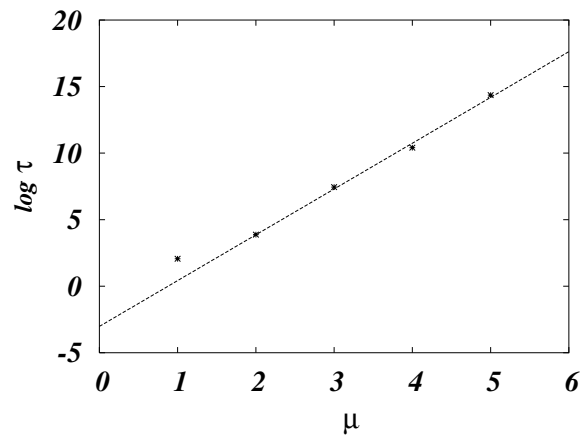


Figure 8. Relaxation times of the diluted spin correlations as a function of the chemical potential in a semi-log plot.

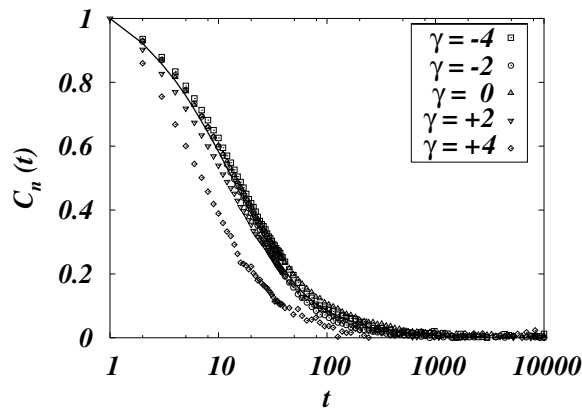


Figure 9. Equilibrium particle correlations $C_n(t)$ for the five possible values of γ_i and $\mu = 3$. The line is the full correlation, from figure 6.

frustrated regions. This may be due to the fact that since particle creation–destruction is allowed, particles appearing in these regions have a higher probability to go elsewhere or be destroyed (as these are regions of less than average densities), which makes the decorrelation time small. On the other hand, low frustration regions are those preferred by the particles and correlations take much more time to decay (as these are regions of larger than average densities). The total correlation (not shown) follows closely the $\gamma_i = 0$ or mean frustration curve. Note that all local correlations show stretched exponential relaxations irrespective of the value of the local frustration being high or low. In this scenario the stretched relaxation does not emerge as a consequence of some kind of convolution of local exponential relaxations with different time scales. At this level of description, the stretching, although heterogeneous due to different local frustration, is intrinsic. As the density increases this scenario does not change qualitatively.

It is interesting to remark that for high values of μ the decay of the diluted spin correlation starts to develop a plateau and the sites responsible for this behaviour are those that are less

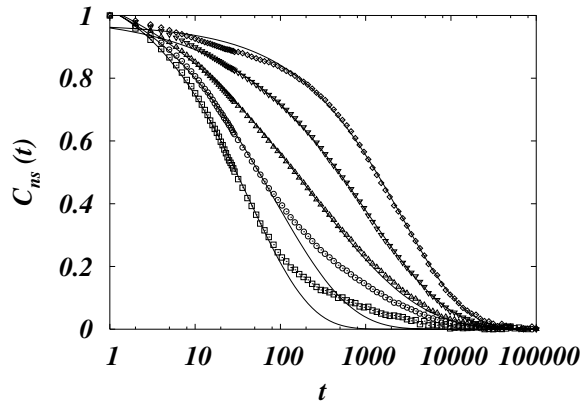


Figure 10. Equilibrium dilute spin correlations $C_{ns}(t)$ for the five possible values of γ_i and $\mu = 3$. The symbols are the same as in figure 9. Note that low frustration sites already show a small plateau, although in the full correlation (figure 7), this is not yet noticeable.

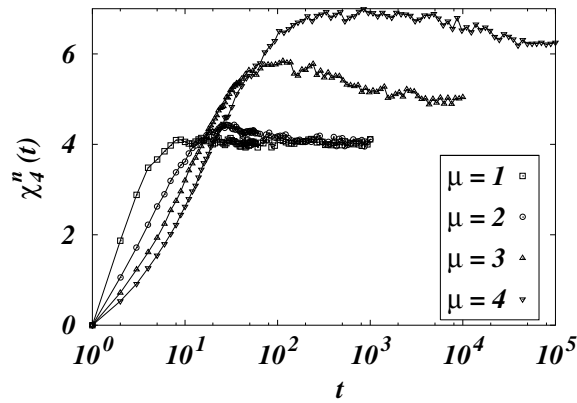


Figure 11. $\chi_4^n(t)$ as a function of time for different chemical potentials. For increasing chemical potential (hence densities) the peak increases and shifts to longer times.

frustrated. The effect is not much pronounced because the summed up effect of $\gamma_i = -2$ and 0 sites is dominant.

As the dynamical heterogeneities have attracted much attention recently, several quantities have been devised to quantify them [4]. Among them, of particular interest is the four point correlation (or dynamical non-linear response) defined as

$$\chi_4^n(t) = N (\langle C_n^2(t) \rangle - \langle C_n(t) \rangle^2). \quad (5)$$

Away from the transition, this function presents a maximum at a time t^* that is a measure of the timescale during which the particles forming the heterogeneity are correlated. The long time behaviour of this quantity is a measure of its equilibrium value. In figure 11 we plot $\chi_4^n(t)$. Analogously to what happens in other glass models it presents a broad peak that shifts to longer times and gets higher as the density increases. Nevertheless, an important difference from other models is that after the peak the non-linear compressibility does not decay too much and develops a density-dependent plateau at long times. The persistence of density correlations is a clear signature of the presence of very long lived heterogeneities,

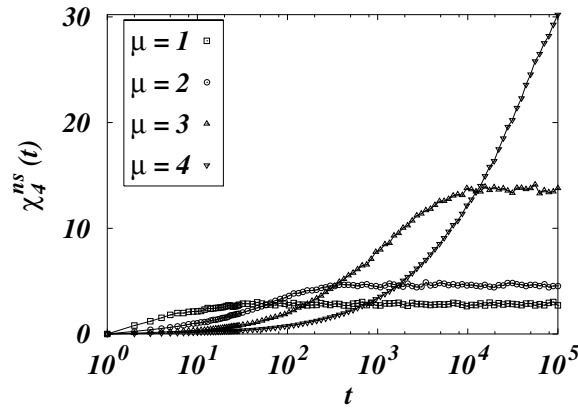


Figure 12. $\chi_4^{ns}(t)$ as a function of time for different chemical potentials. Note here the saturation after a crossover time and the stronger growth of the subsequent plateau at variance with the behaviour of $\chi_4^n(t)$ in figure 11.

a consequence of the pinning effect of the quenched disorder present in the model. The possible divergence of the equilibrium (infinite time) limit of the non-linear compressibility should point to the existence of a thermodynamic transition associated with the density degrees of freedom not yet observed in this model.

Analogously, for diluted spin correlations we can evaluate equation (5) using $C_{ns}(t)$ in the place of $C_n(t)$. The resultant $X_4^{ns}(t)$ is seen in figure 12. The behaviour is similar to that observed for the density variables, but instead of a peak we observe a crossover time after which this non-linear susceptibility saturates in a finite density-dependent value. In this case the height of the plateau seems to diverge much more rapidly than for the compressibility giving more plausibility to the presence of a thermodynamic transition in the spin variables, probably for $\mu \rightarrow \infty$. The crossover to a plateau, instead of the presence of a peak, clearly points to the appearance of a persistent correlation length associated with the spin degrees of freedom. It would be interesting to check if these persistence are a manifestation of a growing structural correlation length which might diverge at an equilibrium spin glass transition similar to that present in $d = 3$.

5. Conclusions

In this paper we considered the role played by heterogeneities present in a model with quenched disorder. Different from self-induced frustration models here the heterogeneities may be pinned by the local frustration and this allows a simple characterization of them. The effects of these pinned heterogeneities on time correlation functions and distribution of local densities have been analysed. The system forms clumps in the liquid phase even when the particles either do not interact or strongly repel each other [28]. Moreover, these clumps are long lived and it would be interesting to study their size distribution and how they are correlated [29].

A simple measure of local frustration was considered and a strong correlation with the inhomogeneous density distribution was found. The use of γ_i allowed to decompose the local density distributions in components related to the degree of local frustration. However, the use of γ_i as a measure of the local frustration considering only the minimal plaquets has to be considered as a first-order approximation. Indeed, higher order plaquets, involving larger loops, have to be taken into account in order to obtain the full dependence of ρ_i on γ_i .

For example, in the $d = 2$ case, there exists 12 plaquets of second order (those having six bonds). It is an open problem to determine to what extent the present results may change by considering the effects of larger loops in γ_i and how they determine the average local density and affect the relaxation properties. It was also shown that dynamic correlations can be decomposed according to the local values of frustration and in each case the relaxations are essentially stretched although the degree of stretching is of course dependent on the degree of local frustration. It would be interesting to study the possible relation between *local* correlation functions in the out-of-equilibrium regime and the violation of the fluctuation–dissipation theorem [16, 30–34] with the local frustration as defined by the parameter γ_i .

Further insight into the relation of the FILG with other models of glasses and spin glasses can be gained by analysing non-linear responses. We showed that two such responses associated with different degrees of freedom in the model behave differently in some important aspects. At variance with models of glasses, the spin non-linear susceptibility shows a crossover time after which the response saturates instead of the characteristic peak observed for example in models with constrained dynamics. Also the rapid growth of the plateau at long times suggests the developing of a structural correlation length associated with a possible spin glass transition. This remains to be confirmed. The non-linear compressibility instead shows a broad peak but with a modest further relaxation to a density-dependent plateau. In this case one can associate this plateau with the formation of very long lived *quenched heterogeneities*. From the observed behaviour of these non-linear responses one can conclude that the FILG does not behave either as a proper spin glass or as a glass sharing some characteristics with both kinds of systems.

Although the model considered here has been originally introduced as an attempt to obtain a finite dimensional lattice system with glassy properties similar to structural glasses, the main drawback is the lack of invariance under spatial translations already in the liquid phase. There are several ways to restore this invariance. For example, by considering spatially coarse-grained variables or by including a temporal evolution of the bonds [22]. As it stands this model still may be interesting to study transport in disordered media (see [35] and references therein) which has been of much interest recently.

Acknowledgments

We acknowledge interesting conversations with Annalisa Fierro and Yan Levin. Work partially supported by the Brazilian agencies FAPERGS and CNPq.

References

- [1] Debenedetti P 1996 *Metastable Liquids, Concepts and Principles* (Princeton: Princeton University Press)
- [2] Debenedetti P G and Stillinger F H 2001 *Nature* **410** 259
- [3] Sastry S, Debenedetti P and Stillinger F 1998 *Nature* **393** 554
- [4] Sillescu H 1999 *J. Non-Cryst. Sol.* **243** 81
- [5] Ediger M D 2000 *Annu. Rev. Phys. Chem.* **51** 99
- [6] Richert R 2002 *J. Phys.: Condens. Matter* **14** R703
- [7] Kob W, Donati C, Plimpton S J, Poole P H and Glotzer S C 1997 *Phys. Rev. Lett.* **79** 2827
- [8] Donati C, Douglas J, Kob W, Plimpton S J, Poole P H and Glotzer S C 1998 *Phys. Rev. Lett.* **80** 2338
- [9] Glotzer S C, Novikov V N and Schroder T B 2000 *J. Chem. Phys.* **112** 509
- [10] Donati C, Franz S, Parisi G and Glotzer S C 2002 *J. Non-Cryst. Sol.* **307–310** 215
- [11] Broderix K, Bhattacharya K K, Cavagna A, Zippelius A and Giardina I 2000 *Phys. Rev. Lett.* **85** 5360
- [12] Angelani L, Leonardo R D, Ruocco G, Scala A and Sciortino F 2000 *Phys. Rev. Lett.* **85** 5356
- [13] Grigera T S, Cavagna A, Giardina I and Parisi G 2002 *Phys. Rev. Lett.* **88** 55502
- [14] Büchner S and Heuer A 2000 *Phys. Rev. Lett.* **84** 2168

-
- [15] Glotzer S, Jan N and Poole P 1998 *Phys. Rev. E* **57** 7350
 - [16] Barrat A and Zecchina R 1999 *Phys. Rev. E* **59** R1299
 - [17] Poole P, Coniglio A, Glotzer S and Jan N 1997 *Phys. Rev. Lett.* **78** 3394
 - [18] Ricci-Tersenghi F and Zecchina R 2000 *Phys. Rev. E* **62** R7567
 - [19] Nicodemi M and Coniglio A 1997 *J. Phys. A: Math. Gen.* **30** L187
 - [20] Lawlor A, Reagan D, McCullagh G D, Gregorio P D and Dawson P T K 2002 *Phys. Rev. Lett.* **89** 245503
 - [21] Dawson K A, Lawlor A, De Gregorio P, McCullagh G D, Zaccarelli E and Tartaglia P 2002 *Physica A* **316** 115
 - [22] Fierro A, de Candia A and Coniglio A 2000 *Phys. Rev. E* **62** 7715
 - [23] Stariolo D A and Arenzon J J 1999 *Phys. Rev. E* **59** R4762
 - [24] Arenzon J J, Ricci-Tersenghi F and Stariolo D A 2000 *Phys. Rev. E* **62** 5978
 - [25] Arenzon J J, Nicodemi M and Sellitto M 1996 *J. Physique I* **6** 1143
 - [26] Crisanti A and Leuzzi L 2002 *Phys. Rev. Lett.* **89** 237204
 - [27] de Candia A and Coniglio A 2001 *Phys. Rev. E* **65** 016132
 - [28] Klein W, Gould H, Ramos R A, Clejan I and Mel'cuk A I 1994 *Physica A* **205** 738
 - [29] Johnson G, Mel'cuk A I, Gould H, Klein W and Mountain R D 1998 *Phys. Rev. E* **57** 5707
 - [30] Castillo H E, Chamon C, Cugliandolo L F and Kennett M P 2002 *Phys. Rev. Lett.* **88** 237201
 - [31] Berthier L 2003 *Preprint cond-mat/0303453*
 - [32] Montanari A and Ricci-Tersenghi F 2003 *Phys. Rev. Lett.* **90** 017203
 - [33] Montanari A and Ricci-Tersenghi F 2003 *Preprint cond-mat/0305044*
 - [34] Castillo H E, Chamon C, Cugliandolo L F, Iguain J L and Kennett M P 2002 *Preprint cond-mat/0211558*
 - [35] Oshanin G, Bénichou O, Burlatsky S F and Moreau M 2003 *Instabilities and Non-Equilibrium Structures IX* ed E Tirapegui and O Descalzi (Dordrecht: Kluwer)